Detection of Early Esophageal Neoplastic Barrett Lesions with Quantified Fluorescence Molecular Endoscopy Using Cetuximab-800CW

Ruben Y. Gabriëls*[1], Lisanne E. van Heijst*[1], Wouter T.R. Hooghiemstra[1], Anne M. van der Waaij[1], Gursah Kats-Ugurlu[2], Arend Karrenbeld[2], Dominic J. Robinson[3], Anna Tenditnaya[4,5], Vasilis Ntziachristos[4,5], Dimitris Gorpas[4,5], and Wouter B. Nagengast[1]

[1]Department of Gastroenterology and Hepatology, University Medical Center Groningen, University of Groningen, Groningen, The Netherlands; [2]Department of Pathology and Medical Biology, University Medical Center Groningen, University of Groningen, Groningen, The Netherlands; [3]Otolaryngology, Center for Optic Diagnostics and Therapy, Erasmus University Medical Center, Rotterdam, The Netherlands; [4]Chair of Biological Imaging at the Central Institute for Translational Cancer Research (TranslaTUM), School of Medicine, Technical University of Munich, Munich, Germany; and [5]Institute of Biological and Medical Imaging, Helmholtz Zentrum München, Neuherberg, Germany

Esophageal adenocarcinoma causes 6% of cancer-related deaths worldwide. Near-infrared fluorescence molecular endoscopy (NIR-FME) uses a tracer that targets overexpressed proteins. In this study, we aimed to investigate the feasibility of an epidermal growth factor receptor (EGFR)–targeted tracer, cetuximab-800CW, to improve detection of early-stage esophageal adenocarcinoma. **Methods:** We validated EGFR expression in 73 esophageal tissue sections. Subsequently, we topically administered cetuximab-800CW and performed high-definition white-light endoscopy (HD-WLE), narrow-band imaging, and NIR-FME in 15 patients with Barrett esophagus (BE). Intrinsic fluorescence values were quantified using multidiameter single-fiber reflectance and single-fiber fluorescence spectroscopy. Back-table imaging, histopathologic examination, and EGFR immunohistochemistry on biopsy samples collected during NIR-FME procedures were performed and compared with in vivo imaging results. **Results:** Immunohistochemical preanalysis showed high EGFR expression in 67% of dysplastic tissue sections. NIR-FME visualized all 12 HD-WLE–visible lesions and 5 HD-WLE–invisible dysplastic lesions, with increased fluorescence signal in visible dysplastic BE lesions compared with nondysplastic BE as shown by multidiameter single-fiber reflectance/single-fiber fluorescence, reflecting a target-to-background ratio of 1.5. Invisible dysplastic lesions also showed increased fluorescence, with a target-to-background ratio of 1.67. Immunohistochemistry analysis showed EGFR overexpression in 16 of 17 (94%) dysplastic BE lesions, which all showed fluorescence signal. **Conclusion:** This study has shown that NIR-FME using cetuximab-800CW can improve detection of dysplastic lesions missed by HD-WLE and narrow-band imaging.

Key Words: Barrett esophagus; cetuximab; epidermal growth factor receptor; esophageal adenocarcinoma; fluorescence molecular imaging

J Nucl Med 2023; 64:803–808
DOI: 10.2967/jnumed.122.264656

Esophageal cancer is responsible for approximately 6% of cancer-related deaths worldwide, with studies predicting a rise in the incidence of esophageal adenocarcinoma (EAC) (*1*). Late-stage detection leads to a 5-y survival rate of 15%–20% (*2*).

Surveillance of Barrett esophagus (BE) is performed by high-definition white-light endoscopy (HD-WLE) and narrow-band imaging (NBI) combined with random biopsies following the Seattle protocol to detect early EAC lesions (*3*). A study performing a follow-up endoscopy procedure 1 y after the primary endoscopy detected 24% more EAC lesions (*4*). This finding indicates a high miss-rate by HD-WLE and NBI in combination with random biopsies during endoscopic surveillance (*4,5*).

In the quest to improve detection of early-stage EAC, near-infrared fluorescence molecular endoscopy (NIR-FME) has recently shown potential to perform better than the current endoscopic standard (*6*). A phase I trial conducted here at the University Medical Center Groningen used the tracer bevacizumab-800CW, targeting vascular endothelial growth factor A, and showed an approximately 33% improvement in early lesion detection compared with conventional HD-WLE and NBI (*7*).

NIR-FME can provide additional guidance in histopathologic assessment and has been shown to reduce sampling error (*8,9*). This technique in combination with the tracer cetuximab-800CW, targeting epidermal growth factor receptor (EGFR), has been described to provide additional real-time information assisting intraoperative decision making aiding tumor delineation (*10*). Recently, multiplexed imaging was successfully introduced in which 2 fluorescently labeled tracers targeting EGFR and human EGFR 2 were evaluated for detection of EAC (*11*).

We validated EGFR expression in BE lesions and aimed to investigate the feasibility of NIR-FME with cetuximab-800CW, an EGFR-targeted tracer, compared with HD-WLE and NBI, to improve detection of early-stage EAC in BE patients.

MATERIALS AND METHODS

This phase I feasibility study with cetuximab-800CW is embedded in an ongoing intervention study performed at the University Medical Center Groningen (NCT03877601). All included patients are priorly diagnosed with low-grade dysplasia (LGD), high-grade dysplasia (HGD),

Received Jul. 13, 2022; revision accepted Dec. 6, 2022.
For correspondence or reprints, contact Wouter B. Nagengast (w.b.nagengast@umcg.nl).
*Contributed equally to this work.
Published online Jan. 5, 2023.

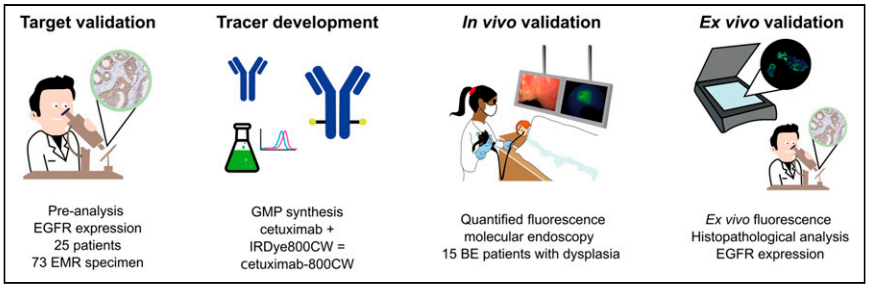

FIGURE 1. Overview of study design. EMR = endoscopic mucosal resection; GMP = good manufacturing practice.

or early-stage EAC at a regional hospital and referred to the University Medical Center Groningen, which is the BE expert center for the northern Netherlands. Included patients underwent HD-WLE combined with an NIR-FME procedure using topical administration of cetuximab-800CW (*12*).

Inclusion and Exclusion Criteria

For the immunohistochemistry preanalysis, we have included esophageal endoscopic mucosal resection specimens of 25 patients. Following all preanalysis study procedures, we selected and included 15 patients eligible for cetuximab-800CW administration. These patients were priorly diagnosed with LGD, HGD, or early-stage EAC and scheduled for an endoscopic procedure. Patients received both oral and written information on study procedures and the tracer. Patients less than 18 y old, allergic to immunoglobulins, pregnant, or breastfeeding were excluded. Additionally, patients who received prior cetuximab treatment, radiation therapy, chemotherapy, immunotherapy, or surgery for esophageal cancer were excluded. All patients interested in participating in either the ex vivo preanalysis or the in vivo procedure with administration of cetuximab-800CW before endoscopy had to give written informed consent within 2 wk but not earlier than 48 h after receiving information. The design of the current study is shown in Figure 1.

Ex Vivo Preanalysis EGFR Expression

Ex vivo preanalysis was performed by 2 independent researchers to investigate EGFR expression. Endoscopic mucosal resection specimens were formalin-fixed for 24 h, and specimens were histologically sectioned into 4-μm tissue slices (n = 73), which were then stained for hematoxylin and eosin, P53, and EGFR. The slices were scanned by a Hamamatsu NanoZoomer (Hamamatsu Photonics) and viewed with NDP.view2 (Hamamatsu Photonics). H-scores were independently calculated in a masked manner by the 2 researchers to quantify EGFR staining intensity.

Synthesis of Cetuximab-800CW

Production of cetuximab-800CW (peak excitation/emission at 778/795 nm) was performed in the cleanroom facility of the Clinical Pharmacy and Pharmacology Department of the University Medical Center Groningen (*12*).

Fluorescence Molecular Endoscopy Combined with Spectroscopy

Real-time in vivo NIR-FME with cetuximab-800CW was achieved by coupling a fiberscope (Schölly Fiberoptic GmbH) to the SurgVision Explorer Endoscope (SurgVision BV), which is based on a system previously developed by our group (*13*).

Multidiameter single-fiber reflectance and single-fiber fluorescence spectroscopy, developed by the University Medical Center Rotterdam, Erasmus MC, was used as a reference for the NIR-FME measurements (*14,15*). The process leading to quantification of tracer's intrinsic fluorescence was previously described (*14,15*). Both NIR-FME and multidiameter single-fiber reflectance/single-fiber fluorescence were performed through the working channel of a standard endoscope.

Procedure

HD-WLE and NBI were performed for general evaluation of the BE segment and suspected lesions. Acetyl cysteine, 0.1%, was used to reduce mucus during the procedure. After a 5-min incubation of the topically administered cetuximab-800CW, the esophagus was rinsed with water to remove abundant, unbound tracer. We administered 1 mL of a 0.1 mg/mL concentration of cetuximab-800CW per 1 cm of BE segment. NIR-FME was performed to examine the esophagus and investigate whether all HD-WLE suspected lesions could be detected and whether additional lesions, missed by HD-WLE/NBI, could be identified. We calculated the target-to-background ratio (TBR): the ratio between the mean NIR-FME image pixel intensities from the region of interest (ROI) (e.g., lesion of fluorescence foci) and the nondysplastic BE (NDBE), determined as the background. The mean value of each ROI was calculated for those pixels within the upper 70% of the corresponding histogram.

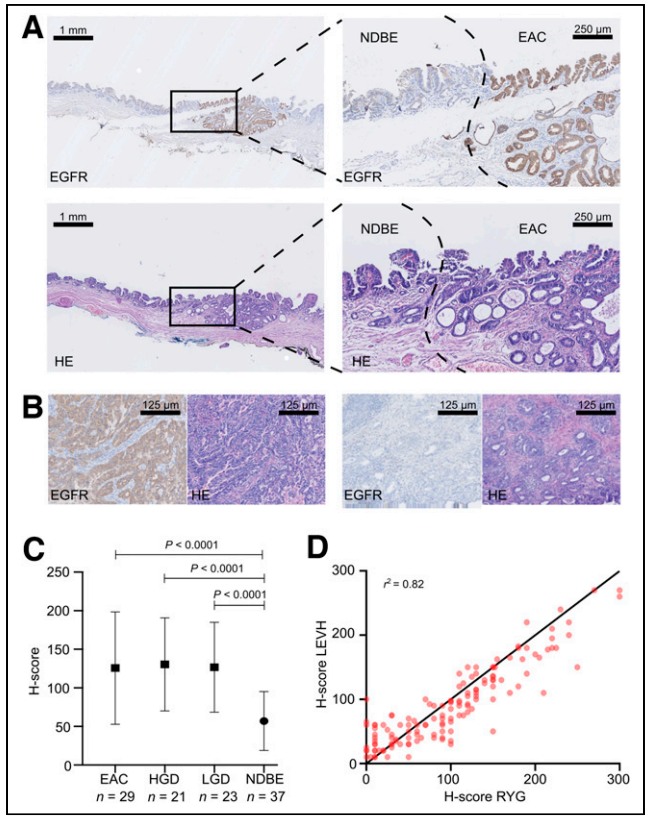

FIGURE 2. (A) Immunohistochemistry results of EGFR staining (brown, top) and hematoxylin and eosin staining (purple, bottom), with pathologic delineation of EAC and NDBE. Left images are at low magnification (×5), and right images are at high magnification (×20). (B) Histopathologic tissue slices at high magnification (×40), with high staining of EAC on left and no staining of EAC on right, showing variable EGFR expression. (C) Mean and SD for H-scoring by 2 independent researchers. (D) Scoring consistency between 2 independent researchers as determined with Pearson correlation coefficient. HE = hematoxylin and eosin.

TABLE 1
Patient Characteristics (n = 15)

Characteristic	Histology				Data
	NDBE	LGD	HGD	EAC	
Male (n)	1 (100%)	2 (100%)	5 (100%)	5 (71.4%)	13 (86.7%)
Mean age (y)	74.5	67.0	64.0	64.2	66
Mean body mass index	28.00	27.10	27.05	27.46	27.43
Lesions identified by referring endoscopist	0	0	1	8	9 (7 patients)
Lesions identified with HD-WLE at BE expert center	0	0	3	9	12 (9 patients)
Additional NIR-FME lesions	0	2	3	0	5 (5 patients)

Five invisible HD-WLE dysplastic lesions were detected using FME.

To assess the quality of the data acquired with the NIR-FME system, we calculated the signal–to–background-noise ratio in decibel scale and the contrast-to-noise ratio for every frame containing visible or invisible lesions (*16*). The reliability of the data was then assessed through the Rose criterion for contrast-to-noise ratio and the 95% confidence level of a measurement for the signal–to–background-noise ratio, which requires a contrast-to-noise ratio of more than 3 and a signal–to–background-noise ratio of more than 6 dB for a lesion to be distinguishable from the background (*17*).

Subsequently, HD-WLE–guided spectroscopy was performed to measure the intrinsic fluorescence of cetuximab-800CW from the NIR-FME–identified suspected or invisible lesions. All measurements were done in triplicate, and mean values were used to quantify cetuximab-800CW fluorescence, serving as control measurements for validation of NIR-FME findings (*18*).

Ex Vivo Analysis

Tissue biopsy samples were collected from unsuspected BE tissue, lesions, and invisible lesions during in vivo NIR-FME procedures. They were then formalin-fixed and paraffin-embedded. From these specimens, 10-μm tissue sections were deparaffinized and imaged with an Odyssey CLx flatbed scanner (LI-COR Biosciences), whereas 4-μm-thick sections were stained with hematoxylin and eosin and P53 and subsequently histopathologically analyzed by 2 pathologists. Immunohistochemistry on EGFR staining was performed on additional 4-μm tissue sections, after which they were scanned by a NanoZoomer (Hamamatsu Photonics) and digitally analyzed using NDP.view2. H-scores were calculated to quantify the staining intensity of EGFR by 2 researchers. A total of 32 formalin-fixed tissue sections stained with EGFR were analyzed.

Statistical Analysis

Analyses and graph layouts were implemented using Prism (version 8.4.2, GraphPad Software Inc.). Normality tests were performed on all data. Descriptive statistics were performed to calculate the mean and SD of the H-scores, and Pearson correlation was used to assess the interobserver agreement of manual H-scoring by the 2 independent researchers. H-scores, TBRs, and in vivo and ex vivo spectroscopy data were analyzed by 1-way ANOVA. P values of less than 0.05 were considered statistically significant. All data are displayed as mean ± SD.

Ethical Considerations

This study was approved by the Medical Ethics Committee at the University Medical Center Groningen (METc number 2018/701).

RESULTS

Ex Vivo EGFR Expression Analysis

In total, 73 formalin-fixed and paraffin-embedded tissue slices were analyzed for EGFR expression levels and histopathology. Two pathologists selected areas containing NDBE, LGD, HGD, and EAC. H-score quantification showed that membranous staining for most of

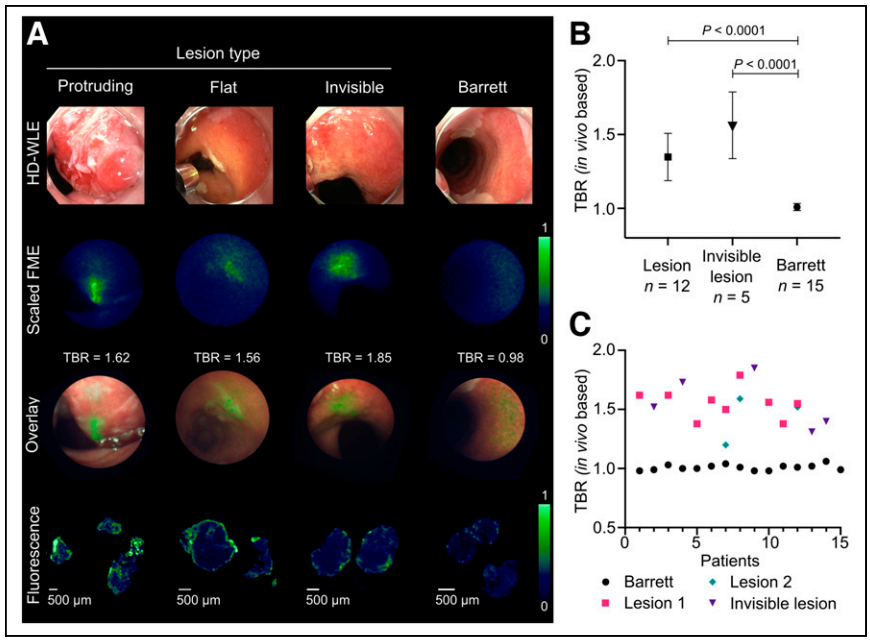

FIGURE 3. (A) Different lesion and tissue types visualized with different imaging techniques. From top to bottom are shown HD-WLE images, corresponding frames acquired with NIR-FME system in fluorescence channel, overlay of color and fluorescence data acquired with NIR-FME, and ex vivo fluorescence images acquired with Odyssey CLx flatbed scanner. Fluorescence images were linearly normalized to common global maximum (1) and minimum (0) values to enable visual comparison of signal strength between different lesion types. (B and C) Calculated TBRs combined and in every single patient separately, respectively.

TABLE 2
Metrics with Corresponding Formulas and Reference Values for Image Quality Assessment

Metric	Formula	Reference value
SNR	$20 \cdot \log 10 \frac{S}{RMSN}$	6 dB
CNR	$\frac{\lvert S-N \rvert}{RMSN}$	1

SNR = signal-to-background noise ratio; S = mean intensity signal; RMSN = root mean square noise calculated as SD from background area; CNR = contrast-to-noise ratio; N = noise calculated as mean background signal.

the dysplastic BE tissue (LGD, HGD, and EAC) were scored intermediate or high (n = 49, 67%) (Fig. 2). However, 24 dysplastic BE tissue areas were scored negatively or low (33%). Subsequently, the H-score for EGFR of NDBE tissue was negative or low in 33 tissue areas (89%). The calculated mean H-score for NDBE was 57 ± 38 and significantly lower than LGD (127 ± 58, $P < 0.0001$), HGD (130 ± 60, $P < 0.0001$), and EAC (126 ± 73, $P < 0.0001$). The fraction of variance between the 2 researchers was calculated with the Pearson correlation coefficient (r = 0.9056) (Fig. 2).

Patient Characteristics

Fifteen patients, 2 of whom were female and 13 male, were included in the trial. All included patients received cetuximab-800CW during the procedure, and none of the patients experienced any serious adverse events. The patient characteristics are shown in Table 1.

NIR-FME

All 9 lesions detected by the referring endoscopist at the regional hospitals were detected by our BE expert endoscopist. Furthermore, our BE expert endoscopist additionally detected 3 flat lesions by HD-WLE that were not described by the referring endoscopist. All 12 HD-WLE–visible lesions were visualized by the NIR-FME camera, showing increased fluorescence intensity. Histopathologic assessment by a BE expert pathologist showed dysplasia in all visible and invisible lesions. We observed a clear ex vivo fluorescence signal on the epithelial side of all biopsy samples in dysplastic lesions.

The TBRs of the complete delineated visible lesions were a mean of 1.3 ± 0.2 ($P <$ 0.0001), whereas the invisible lesions presented a higher mean TBR of 1.6 ± 0.2 ($P <$ 0.0001). We could not detect a lesion using either HD-WLE or the NIR-FME system in 1 patient referred with LGD, and additional random biopsies according to the Seattle protocol did not detect dysplasia either. The distribution of mean TBRs per tissue and per patient is shown in Figure 3. Data quality assessment showed an average signal–to–background-noise ratio of 21.79 ± 1.65 dB and an average contrast-to-noise ratio of 4.54 ± 1.57, both being above the corresponding critical values for discrimination between lesion and background, as defined in Table 2.

In 5 patients, NIR-FME detected areas that did not show morphologic changes suggestive of dysplasia by HD-WLE or NBI. These areas showed dysplasia on histology and thus counted as invisible lesions by standard imaging technology (Fig. 4).

In Vivo Multidiameter Single-Fiber Reflectance/Single-Fiber Fluorescence Spectroscopy

Multidiameter single-fiber reflectance/single-fiber fluorescence spectroscopy measurements were performed to quantify the intrinsic fluorescence values of the tracer in vivo by correcting for optical properties of the tissue. Measurements of NDBE were completed for all patients, with the tracer showing a mean intrinsic fluorescence of 0.012 ± 0.003 $Q \cdot \mu_{a,x}^{f}$. The mean value for visible lesions (n = 10) was calculated from 30 measurements and was higher, at 0.018 ± 0.004 $Q \cdot \mu_{a,x}^{f}$, than for NDBE (P = 0.0014), with a spectroscopy TBR of 1.5. These findings are comparable to the in vivo analysis of the raw fluorescence images. In vivo spectroscopy measurements were not feasible for 2 lesions. In one, it was impossible to perform reliable measurements because the spectroscopy fiber was angled toward the lesion. In the other, the spectroscopy measurements failed because we had unstable contact between the lesion and the fiber. Invisible lesions (n = 5) showed a higher mean of 0.020 ± 0.005 $Q \cdot \mu_{a,x}^{f}$ than did NDBE (P = 0.0003). This results in a calculated spectroscopy TBR of 1.67, confirming the data from the in vivo raw fluorescence image analysis of HD-WLE–invisible lesions. In vivo spectroscopy results are shown in Figure 5.

Ex Vivo EGFR Expression

All 17 dysplastic esophageal lesions showed a moderate to strong ex vivo fluorescence signal. LGD was found in 2 tissue slices, HGD in 6 tissue slices, and EAC in 9 tissue slices. NDBE was found in 15 tissue slices collected from endoscopically unsuspected BE tissue. Examples of EGFR expression levels in the samples are shown in Figure 6. H-score quantification showed that in 94% of dysplastic BE tissue (LGD, HGD, and EAC) collected from visible and invisible lesions, epithelial EGFR staining was scored intermediate or high. NDBE tissue showed an ex vivo negative

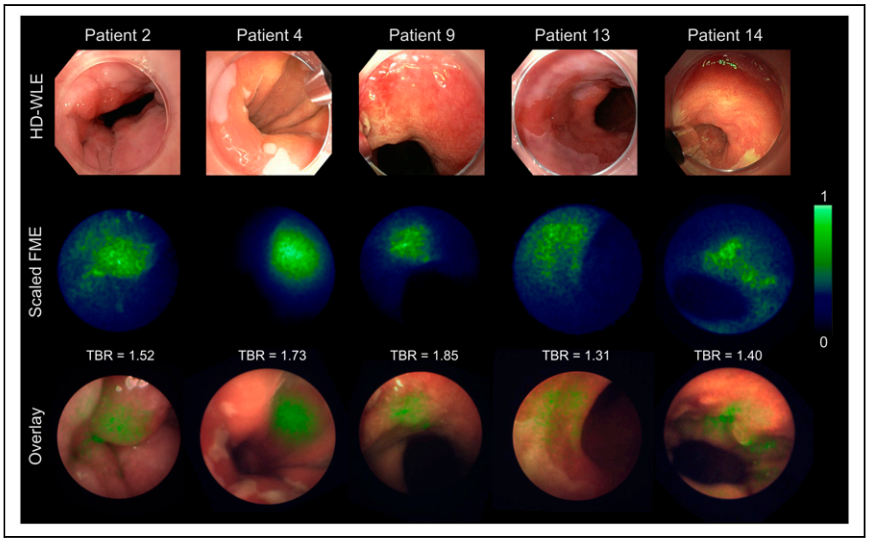

FIGURE 4. HD-WLE–invisible dysplastic lesions detected by NIR-FME. From top to bottom are shown HD-WLE images, corresponding NIR-FME fluorescence images of HD-WLE–invisible lesions, and overlay of NIR-FME color and fluorescence data from 5 different patients. All fluorescence images were normalized with regard to their individual maximum (1) and minimum (0) values to enable visual assessment of fluorescence localization.

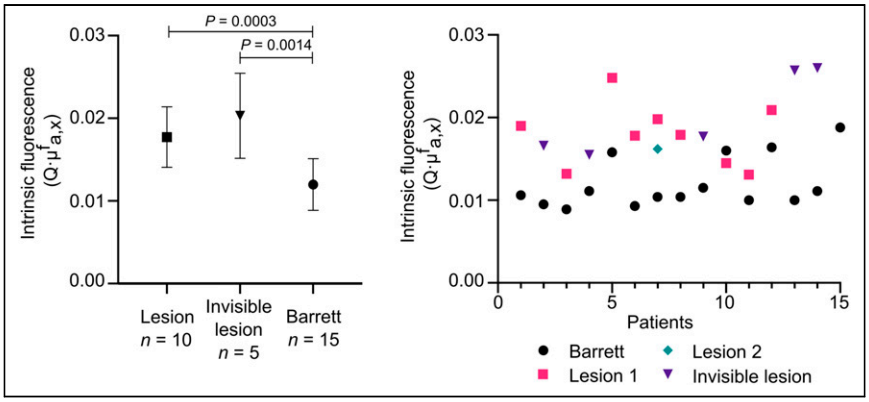

FIGURE 5. In vivo spectroscopy results. (Left) In vivo spectroscopy differences between HD-WLE–visible lesions, HD-WLE–invisible lesions, and NDBE. (Right) In vivo spectroscopy fluorescence values for NDBE, HD-WLE–visible lesions, and HD-WLE–invisible lesions within each patient.

fluorescence signal and lower EGFR expression H-score results than HGD and EAC tissue.

DISCUSSION

Early detection of dysplastic BE and early-stage EAC can prevent progression toward locally advanced EAC and thereby improve morbidity and mortality rates significantly. In the current study, we investigated EGFR expression in dysplastic BE and early-stage EAC tissue. Furthermore, we tested the safety and feasibility of cetuximab-800CW in vivo to improve malignant and premalignant esophageal lesion detection with NIR-FME in BE. Our immunohistochemistry preanalysis showed intermediate to high EGFR expression within 67% of the dysplastic areas. NIR-FME with cetuximab-800CW detected all visible dysplastic lesions and additionally revealed 5 dysplastic lesions missed using HD-WLE/NBI. The specificity of the results was confirmed by 2 independent BE expert pathologists, and 16 of the 17 dysplastic lesions (94%) showed intermediate or high EGFR expression levels. This finding signifies the ability of cetuximab-800CW to visualize dysplastic areas in BE even if morphologic abnormalities cannot be detected by HD-WLE/NBI.

Results from our previous in vivo feasibility study with the tracer bevacizumab-800CW showed that NIR-FME could improve early lesion detection significantly (*7*). Another published phase I proof-of-concept study demonstrated the feasibility of using an EGFR-targeted tracer in combination with a tracer targeting human EGFR 2 for the detection of early EAC lesions using dual-channel spectral endoscopic imaging (*11*). However, EGFR or human EGFR 2 expression analysis was not performed, and in vivo imaging results were not quantified (*11*). The follow-up clinical trial showed an in vivo TBR of 1.5 using an EGFR-targeted tracer in 31 patients, although additional lesions were not detected (*19*). In our phase I clinical trial, we found that the EGFR-targeted tracer cetuximab-800CW detected all known dysplastic lesions and, more importantly, detected 5 invisible dysplastic lesions confirmed by histopathology, which were also shown to be EGFR-positive. Quantified NIR-FME improves early lesion detection by 29% over the current clinical standard using HD-WLE/NBI endoscopy. We quantified EGFR expression in an extensive preanalysis in esophageal endoscopic mucosal resection specimens and subsequently in all esophageal biopsy samples taken during the NIR-FME procedure. Moreover, we confirmed our in vivo NIR-FME findings with unbiased spectroscopy measurements.

Our ex vivo analysis regarding the biopsies showed relatively high EGFR expression within dysplastic esophageal tissue. One reason for these higher EGFR expression levels than reported in the literature might be our relatively small patient sample size from the phase 1 trial in which we analyzed EGFR expression. All 17 NIR-FME–identified lesions, HD-WLE–visible and HD-WLE–invisible, showed in vivo fluorescence after incubation with cetuximab-800CW, suggesting that when lesions are EGFR-positive, they can be detected by cetuximab-800CW. However, 1 lesion did not show clear EGFR expression in the ex vivo analysis, possibly because of sampling error during biopsy.

Fluorescence molecular imaging can be further developed and improved by addressing several study limitations. We included solely referred BE patients with a suspected lesion. Consequently, our cohort consisted mainly of patients with EAC, resulting in a distorted representation of the overall BE population. Research has shown that endoscopists at regional, non–BE expert, centers detect significantly fewer EAC lesions than endoscopists at a BE expert center (*20*). Therefore, we most likely detected more suspected lesions using HD-WLE than did referring centers, potentially indicating that this novel red flag imaging technique is of even greater value for regional, non–BE expert, centers. It would be of great interest to include non–BE experts in a follow-up study to evaluate the impact of this technique. We manually calculated the TBRs from in vivo images by comparing the fluorescence signal of the region for the area of interest with the unspecific fluorescence signal of a region for NDBE. A reason for these relatively low TBRs could be the heterogeneous distribution of the topically administered tracer. Another limitation is that we could not visualize the tracer on a microscopic level. The obtained biopsy samples were directly formalin-fixed after the endoscopic procedure. Our previous study with bevacizumab-800CW demonstrated that the tracer is almost entirely washed away during paraffin embedding, resulting in a loss of fluorescence signal (*13*). However, in the best

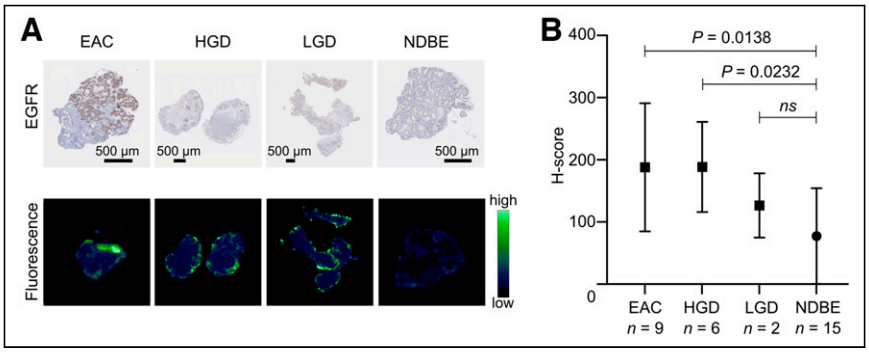

FIGURE 6. EGFR expression and ex vivo fluorescence in different tissue types. (A) Tissue slices with EGFR staining (top) and corresponding deparaffinized tissue slices scanned with Odyssey CLx flatbed scanner, showing fluorescence at luminal side of tissue where tracer was sprayed (bottom). (B) Calculated H-score of EGFR staining.

possible manner, ex vivo images made with the Odyssey CLx fluorescence flatbed scanner showed a clear signal only on the luminal side of the tissue. Finally, we could not take real-time spectroscopy measurements. All measurements were calculated and analyzed after completion of all study procedures. Since we needed the endoscopic working channel for both the fluorescence molecular endoscope and the spectroscopy fibers, we could not measure the intrinsic fluorescence and search for the most intensely fluorescent spot simultaneously. This limitation might explain why the measured fluorescence signal was not higher in the lesion than in the background in one of the included patients.

Over the last few years, several new imaging techniques have been developed to improve early EAC lesion detection in BE patients. Among them are computer-aided diagnosis algorithms (*21*), which might be used as a second assessor. Computer-aided diagnosis already performs better at EAC detection than general endoscopists with HD-WLE images alone, showing a sensitivity of 93% versus 72% and a specificity of 83% versus 74% (*22*). We envision that HD-WLE and FME assisted by computer-aided diagnosis can further improve detection of early EAC lesions, with the aim of making the Seattle protocol redundant and improving patient outcome.

CONCLUSION

We validated that EGFR is overexpressed in malignant and premalignant esophageal tissue. We demonstrated in vivo that this novel red flag imaging technique in combination with cetuximab-800CW has potential to improve early lesion detection in BE patients. We expect that a dual-channel spectral imaging study using an EGFR-targeted tracer in combination with a vascular endothelial growth factor A–targeted tracer can further improve detection of early malignant and premalignant lesions in these patients.

DISCLOSURE

This project has received funding from the European Union's Horizon 2020 research and innovation programme under grant agreement no. 643638 (TRANSCAN-2; project ESCEND) as well as the Dutch Cancer Society, Amsterdam, the Netherlands and the Bundesministerium für Bildung und Forschung (BMBF), Bonn, Germany (FKZ 01KT1809).

KEY POINTS

QUESTION: Does NIR-FME in combination with cetuximab-800CW, an EGFR-targeted tracer, improve detection of early-stage EAC.

PERTINENT FINDINGS: This study adds an extensive ex vivo validation of EGFR expression in dysplastic and nondysplastic esophageal tissue to gain insight into the variability of this expression. In vivo, we additionally detected 5 HD-WLE–invisible lesions, further quantified in vivo fluorescence results with spectroscopy, and validated these results ex vivo with EGFR expression levels.

IMPLICATIONS FOR PATIENT CARE: Dual-channel spectral NIR-FME including an EGFR-targeted tracer will further improve detection of malignant and premalignant lesions in the esophagus.

REFERENCES

1. Sung H, Ferlay J, Siegel RL, et al. Global Cancer Statistics 2020: GLOBOCAN estimates of incidence and mortality worldwide for 36 cancers in 185 countries. *CA Cancer J Clin.* 2021;71:209–249.
2. Alsop BR, Sharma P. Esophageal cancer. *Gastroenterol Clin North Am.* 2016;45:399–412.
3. Sharma P, Hawes RH, Bansal A, et al. Standard endoscopy with random biopsies versus narrow band imaging targeted biopsies in Barrett's oesophagus: a prospective, international, randomised controlled trial. *Gut.* 2013;62:15–21.
4. Visrodia K, Singh S, Krishnamoorthi R, et al. Magnitude of missed esophageal adenocarcinoma after Barrett's esophagus diagnosis: a systematic review and meta-analysis. *Gastroenterology.* 2016;150:599–607.e7.
5. van Putten M, Johnston BT, Murray LJ, et al. 'Missed' oesophageal adenocarcinoma and high-grade dysplasia in Barrett's oesophagus patients: a large population-based study. *United European Gastroenterol J.* 2018;6:519–528.
6. de Boer E, Harlaar NJ, Taruttis A, et al. Optical innovations in surgery. *Br J Surg.* 2015;102:56–72.
7. Nagengast WB, Hartmans E, Garcia-Allende PB, et al. Near-infrared fluorescence molecular endoscopy detects dysplastic oesophageal lesions using topical and systemic tracer of vascular endothelial growth factor A. *Gut.* 2019;68:7–10.
8. Lee YJ, Krishnan G, Nishio N, et al. Intraoperative fluorescence-guided surgery in head and neck squamous cell carcinoma. *Laryngoscope.* 2021;131:529–534.
9. Warram JM, de Boer E, van Dam G, et al. Fluorescence imaging to localize head and neck squamous cell carcinoma for enhanced pathological assessment. *J Pathol Clin Res.* 2016;2:104–112.
10. Morlandt AB, Moore LS, Johnson AO, et al. Fluorescently labeled cetuximab-IRDye800 for guided surgical excision of ameloblastoma: a proof of principle study. *J Oral Maxillofac Surg.* 2020;78:1736–1747.
11. Chen J, Jiang Y, Chang TS, et al. Multiplexed endoscopic imaging of Barrett's neoplasia using targeted fluorescent heptapeptides in a phase 1 proof-of-concept study. *Gut.* 2021;70:1010–1013.
12. Linssen MD, Ter Weele EJ, Allersma DP, et al. Roadmap for the development and clinical translation of optical tracers cetuximab-800CW and trastuzumab-800CW. *J Nucl Med.* 2019;60:418–423.
13. Glatz J, Varga J, Garcia-Allende PB, Koch M, Greten FR, Ntziachristos V. Concurrent video-rate color and near-infrared fluorescence laparoscopy. *J Biomed Opt.* 2013;18:101302.
14. Koller M, Qiu SQ, Linssen MD, et al. Implementation and benchmarking of a novel analytical framework to clinically evaluate tumor-specific fluorescent tracers. *Nat Commun.* 2018;9:3739.
15. Hoy CL, Gamm UA, Sterenborg HJCM, Robinson DJ, Amelink A. Method for rapid multidiameter single-fiber reflectance and fluorescence spectroscopy through a fiber bundle. *J Biomed Opt.* 2013;18:107005.
16. Bao Q, Chatziioannou AF. Estimation of the minimum detectable activity of preclinical PET imaging systems with an analytical method. *Med Phys.* 2010;37:6070–6083.
17. Cherry SR, Sorenson JA, Phelps ME. *Physics in Nuclear Medicine.* Elsevier; 2012:244.
18. van Leeuwen–van Zaane F, Gamm UA, van Driel PB, et al. *In vivo* quantification of the scattering properties of tissue using multi-diameter single fiber reflectance spectroscopy. *Biomed Opt Express.* 2013;4:696–708.
19. Chen J, Yang J, Chang TS, et al. Detection of Barrett's neoplasia with near-infrared fluorescent heterodimeric peptide. *Endoscopy.* 2022;54:1198–1204.
20. Schölvinck DW, van der Meulen K, Bergman JJGHM, Weusten BLAM. Detection of lesions in dysplastic Barrett's esophagus by community and expert endoscopists. *Endoscopy.* 2017;49:113–120.
21. van Heijst LE, Zhao X, Gabriëls RY, Nagengast WB. Today's mistakes and tomorrow's wisdom in endoscopic imaging of Barrett's esophagus. *Visc Med.* 2022;38:182–188.
22. de Groof AJ, Struyvenberg MR, van der Putten J, et al. Deep-learning system detects neoplasia in patients with Barrett's esophagus with higher accuracy than endoscopists in a multistep training and validation study with benchmarking. *Gastroenterology.* 2020;158:915–929.e4.